

## The joint effect of doping with tin(IV) and heat treatment on the transparency and conductivity of films based on titanium dioxide as photoelectrodes of sensitized solar cells

Svetlana Kuznetsova<sup>1,a</sup>, Olga Khalipova<sup>1</sup>, Yu-Wen Chen<sup>2</sup>, Vladimir Kozik<sup>1</sup>

<sup>1</sup>National Research Tomsk State University, Tomsk, 634050 Russia

<sup>2</sup>National Central University, Jhongli, 32001, Taiwan

<sup>a</sup>onm@mail.tsu.ru

Corresponding author: Svetlana Kuznetsova, onm@mail.tsu.ru

**ABSTRACT** This study focuses on the preparation of transparent conducting TiO<sub>2</sub> films with the addition of Sn(IV) by sol-gel method from film-forming solutions based on n-C<sub>4</sub>H<sub>9</sub>OH-(C<sub>4</sub>H<sub>9</sub>O)<sub>4</sub>Ti-SnCl<sub>4</sub>·5H<sub>2</sub>O at the temperature of 300–400 °C. Such films attract great attention because they can be used in flexible transparent photoanodes for the preparation of high effective sensitized solar cells. The morphology, phase composition, and optical properties of films were studied by X-ray diffraction, X-ray spectral microanalysis, scanning electron microscopy, spectrophotometry, and ellipsometry. The content of Sn(IV) influences the composition of films. The solid solution based on titanium dioxide with anatase structure is formed at a content of 5 mol.% Sn(IV); the films with a content of 10–30 mol.% Sn(IV) are the mixture of the TiO<sub>2</sub>:Sn solid solution and SnO<sub>2</sub> with rutile structure. Regardless of the tin content, all films contain an amorphous TiO<sub>2</sub>·nH<sub>2</sub>O phase. The formation of oxide phases occurs through the stages of thermal destruction of Sn(OH)<sub>3</sub>Cl, tin acid, and burnout of butoxy groups of butoxytitanium(IV). The as-synthesized oxide films are uniform and continuity regardless of the tin content. An increase in the content of Sn(IV) in the composition of the films leads to an increase in their thickness from 48 to 105 nm and a decrease in the refractive index from 1.89 to 1.66. The minimum resistance value is characteristic for films that are the solid solution with an anatase structure and with an admixture of the amorphous phase of titanous acid. The surface resistance of the glass decreases by 10<sup>8</sup> times after deposition of the film based on TiO<sub>2</sub> with 5 mol.% Sn(IV). Films based on TiO<sub>2</sub> with 5 mol.% Sn(IV) are characterized by a higher transparency coefficient in the entire visible range of the spectrum (80–70%) and can be used in photoelectrode in dye-sensitized solar cells.

**KEYWORDS** film-forming solution, oxide composite film, tin oxide, titanium oxide, sol-gel method.

**ACKNOWLEDGEMENTS** This work was carried out within the framework of project No 18-29-11037 of Russian Foundation for Basic Research.

**FOR CITATION** Kuznetsova S., Khalipova O., Yu-Wen Chen, Kozik V. The joint effect of doping with tin(IV) and heat treatment on the transparency and conductivity of films based on titanium dioxide as photoelectrodes of sensitized solar cells. *Nanosystems: Phys. Chem. Math.*, 2022, **13** (2), 192–203.

### 1. Introduction

Driven by the growing threat of energy crisis, the use of solar energy is one of the most remarkable approaches for renewable natural resources utilization. It is inducing the scientific community to make great efforts towards the direction of improving solar energy conversion technologies. One of the main trends in modern solar energy is the creation of non-silicon photovoltaic devices. The great interested device of the last generation is the dye-sensitized solar cell (DSSC), being a low-cost and high-efficiency solar energy-to-electricity converter. The DSSCs may represent a cost-effective alternative to traditional silicon solar cells which have a number of disadvantages such as high cost, the need for a large area of the battery itself, as well as low efficiency in geographic areas with a large amount of precipitation [1–3]. The light absorption and the charge carrier transport are separated in DSSCs, which allow one to improve the performance of the device by optimizing each process separately. Moreover, the technology of DSSC allows creating the flexible solar cells. In such photovoltaic devices, wide-gap semiconductors are used as a photoanode.

A lot of research has been done on titanium dioxide electrodes [4, 5], but the efficiency of these dye-sensitized solar cells was only 12.3% which is much lower than that of solar cells produced by silicon technology [6, 7]. Thus, it is an urgent task to search for new approaches to the production of photoanodes based on thin oxide films for high-efficiency DSSCs. One of the ways is a modification of titanium dioxide by tin dioxide. Tin dioxide is one of the most studied metal oxide semiconductor, which has attracted a great deal of attention in the field of solar cells and photocatalysis due to its excellent optical properties, high stability of its photochemical properties, quick recombination of photo-generated

charge carriers, large band gap ( $E_g = 3.6$  eV), high electron mobility ( $125 \text{ cm}^2\text{V}^{-1}\text{s}^{-1}$ ) [8–14]. Moreover, the  $\text{SnO}_2$  can act itself as a photoanode replacing titanium dioxide. Previous research showing the possibility of using tin dioxide as an electronically conductive transparent layer have appeared quite recently. Li et al. [15] were one of the first researchers who developed solar cells with such photoanodes. However, the highest power conversion efficiency of these devices was less than 3.8%. Later, Ke et al. [16] obtained the oxide film from a tin(II) chloride solution and prepared the photoanode with an average efficiency of 16.0%. In addition, according to the literature [17, 18], the use of a  $\text{TiO}_2/\text{SnO}_2$  bilayer as an effective layer for extracting electrons makes it possible to increase power conversion efficiency of perovskite solar cell device up to 18.85% compared to the individual  $\text{TiO}_2$ .

There are many previous reports available about the preparation of  $\text{TiO}_2$  and  $\text{SnO}_2$  films using not expensive, simple chemical methods such as sol-gel method. Most of the works performed earlier show that the synthesis temperature of conductive and transparent tin dioxide by the sol-gel method from film-forming solutions (FFSs) should be at least 500–600 °C, since at this temperature crystalline phase of tin oxide is formed [19, 20]. The production of crystalline titanium dioxide also requires high temperatures [21]. This is a serious obstacle to the use of  $\text{TiO}_2$  and  $\text{SnO}_2$  films on flexible transparent photoanodes that can withstand temperatures of 200–300 °C. Some research groups propose to obtain  $\text{TiO}_2$  films with  $\text{SnO}_2$  at temperatures of 400–500 °C from sols based on organic derivatives of titanium(IV), and tin(II) or tin(IV) chloride. For example, in work [22], films were obtained from sols based on titanium(IV) n-butoxide and tin(II) chloride in ethanol at 450 °C. The authors of this work claim the formation of a solid solution based on titanium dioxide up to 30 mol.% tin. The same composition was indicated by the authors of the work [23], in which films based on titanium dioxide and tin dioxide were obtained from isopropanol-based sols with titanium isopropoxide, and tin(II) chloride. However, very wide diffraction maxima and modes in the Raman spectra, which are presented in these works, indicate the presence of an amorphous phase in these samples, the composition of which is unknown. Moreover, there are no data in the literature that make it possible to evaluate the possibility of using the sol-gel method to obtain the transparent conducting films of titanium dioxide with the addition of tin(IV) at temperatures below 450 °C.

In this present study, the transparent conducting  $\text{TiO}_2$  films with the addition of tin(IV) was obtained by sol-gel method from FFSs based on  $n\text{-C}_4\text{H}_9\text{OH}-(\text{C}_4\text{H}_9\text{O})_4\text{Ti-SnCl}_4 \cdot 5\text{H}_2\text{O}$  at temperatures of 300–400 °C and the process of obtaining films was researched. As a consequence of this systematic study, we established that the composition of films obtained at temperatures of 300–400 °C differs depending on the content of tin(IV). A comparative study of optical properties of films with different compositions and preparing temperatures have also been made. It was found that it is possible to obtain transparent conducting films of titanium dioxide with the addition of tin(IV) at temperatures below 450 °C by sol-gel method, indicating the considerable potential for application in high-efficiency solar converter.

## 2. Experimental part

### 2.1. Preparation of $\text{TiO}_2$ with Sn(IV) composite films on glass substrates

Films based on titanium dioxide with Sn(IV) additive (1–30 mol.% Sn(IV)) were obtained by the sol-gel method from FFSs based on titanium(IV) n-butoxide (TBT) and tin(IV) chloride in butanol-1. The starting reagents were butanol-1 (AO "EKOS-1", Russia, reagent purity 99,9 wt. %), titanium(IV) n-butoxide (TBT) ("Acros Organic, USA, reagent purity 99,9 wt. %),  $\text{SnCl}_4 \cdot 5\text{H}_2\text{O}$  (Neftegazkhimkoplect, Russia, reagent purity 99 wt. %). Laboratory glass slides  $2.0 \pm 0.2$  mm (Russia) were used as the substrates.

The FFSs were obtained at room temperature by dissolving a crystalline hydrate of tin(IV) chloride and then TBT in butanol-1. The amounts of substances were such that the total molar concentration of tin(IV) chloride and TBT was 0.3 mol/L. The FFSs were applied to glass substrates by dip-coating at a rate of 3 mm/min. The device consisted of a clamp for the substrate, a speed controller for dip-coating, and a little table on which the cuvette with FFSs are placed. After the application of FFSs on glass substrates, the samples were dried in a SNOL58/350 LEN drying oven at a temperature of 60 °C (FFS 60 °C) for one hour and annealed in a PM-1.0-20 muffle furnace at 300, or 400 °C for 1 and 9 hours.

### 2.2. Methods for studying film-forming solutions and $\text{TiO}_2$ with Sn(IV) composite films

The composition of the FFSs and the processes occurring in them were investigated by IR spectroscopy and viscometry. The IR spectra of the samples were carried out on a Nicolet 6700 spectrophotometer (USA) in the frequency range from 400 to 4000  $\text{cm}^{-1}$ . The viscosity of the FFSs was determined using a VPZh-2 (Russia) capillary viscometer with a capillary diameter of 0.73  $\text{mm}^3$ . The capillary viscometer consisted of one capillary with a funnel and a narrow tube. The assessment of the viscosity was carried out by measuring the time during which a certain volume of the investigated FFS flows out of the funnel. The kinematic viscosity was calculated using the following formula:

$$\eta = \left( \frac{g}{9.807} \right) \cdot \tau \cdot K \quad (1)$$

where  $\eta$  is kinematic viscosity of the liquid,  $\text{mm}^2/\text{s}$ ;  $\tau$  is time of liquid flow, s;  $g$  is acceleration due to gravity,  $\text{m}/\text{s}^2$ ; and  $K$  is viscometer constant,  $\text{mm}^2/\text{s}^2$ . The average size of colloidal particles in the FFSs was determined by the "turbidity spectrum" method. The method is based on the use of the Rayleigh equation for colloidal systems with low concentration,

the dispersed phase of which doesn't absorb incident light and is optically isotropic [24]. The absorption spectra of FFSs in the visible and ultraviolet regions were recorded relative to air on a PE-5400 UV spectrophotometer (Russia).

The thermal decomposition of the butanol-1-TBT-SnCl<sub>4</sub>·5H<sub>2</sub>O film-forming solution containing 20 mol.% Sn(IV) was studied by thermal analysis and IR spectroscopy. Before analysis, solution was dried at 60 °C until the formation of dry residue. The obtained sample was denoted as FFS-60(20 mol.% Sn(IV)). For comparison, the thermal decomposition of the dry (drying at 60 °C) residue of butanol-1-TBT and butanol-1-SnCl<sub>4</sub>·5H<sub>2</sub>O solution was also investigated. Synchronous thermal analysis was conducted using an STA 449 F1 Jupiter thermoanalyzer (Netzsch-Gertebau GmbH, Germany).

The phase composition of the composites based on titanium dioxide with tin(IV) additive was determined by X-ray diffraction (XRD) using a Rigaku Miniflex 600 diffractometer (Rigaku, Japan) with CuK<sub>α</sub> radiation in the 2θ range from 10 to 80°. The diffraction pattern was scanned by steps of 0.02 and a recording rate of 2 deg/min. The resulting diffractograms were interpreted using the JCPDS-ICDD diffraction database. The morphology of the composites was studied by scanning electron microscopy (SEM). The distribution of the elements on the surface was determined based on energy-dispersive X-ray spectroscopic (EDX) analysis. It was performed on a Hitachi TM-3000 scanning electron microscope with a ShiftED 3000 electron microprobe (Hitachi High-Technologies Corporation, Japan). The transmittance of the investigated composite films on the glass in the visible region of the spectrum was studied on a PE5400UF spectrophotometer in the wavelength range of 340–1000 nm. Pure glass was used as a reference sample. The thicknesses and refractive indexes of the composite materials were investigated by the ellipsometry method using SE400 (Germany) and LEF-3M (Russia) ellipsometers. Surface resistance was measured by the two-probe method. The surface resistance of the samples was measured from room temperature to 200 °C. The activation energy of charge carriers was calculated from the tangent of the angle of inclination of the tangent as follows:

$$\operatorname{tg} \alpha = \frac{\Delta \log(1/R)}{\Delta(1/T)}, \quad (2)$$

$$E_a = \frac{2 \tan \alpha R}{0.43}, \quad (3)$$

where  $R = 8.314 \text{ J/mol}\cdot\text{K}$ .

### 3. Results and discussion

#### 3.1. Composition and properties of film-forming solutions based on Butanol-1-TBT-SnCl<sub>4</sub>·5H<sub>2</sub>O

The IR spectra of FFSs with different ratios of TBT and tin(IV) chloride (Fig. 1) have the same set of absorption frequencies for different bond vibrations, which slightly differ in the absorption coefficient.

The observed absorption bands were assigned based on the literature data [25,26]. An analysis of the obtained spectra showed that the FFSs contain hydroxyl groups (the broad peak with a maximum at a frequency of 3921 cm<sup>-1</sup>), methyl and methylene groups (the stretching vibrations at 2958, 2931, and 2872 and bending vibrations at 1457 cm<sup>-1</sup>) of butanol and butoxy groups of TBT. The absorption bands at frequencies of 1009, 951, and 512 cm<sup>-1</sup> correspond to the vibrations of Ti-OH, O-Ti-O, and Ti-O bonds. The band at a frequency of 822.4 cm<sup>-1</sup> corresponds to the vibration of the Sn-O bond. The results of IR spectroscopy indicate that hydrolysis of TBT and SnCl<sub>4</sub> occurs in butanol with the participation of crystallization water introduced into butanol together with SnCl<sub>4</sub>·5H<sub>2</sub>O.

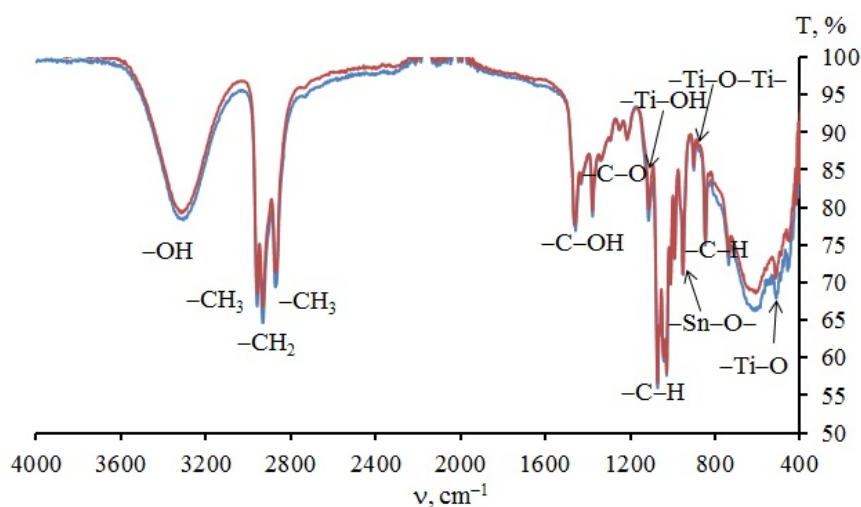
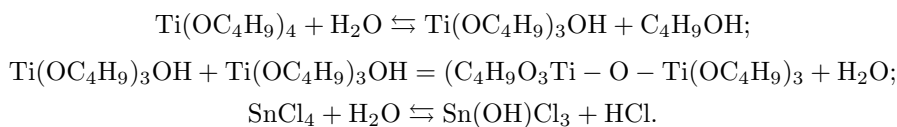


FIG. 1. IR spectra of FFSs based on Butanol-1-TBT-SnCl<sub>4</sub>·5H<sub>2</sub>O with the Sn(IV) content of 1 mol.% (red curve) and 5 mol.% (blue curve)

The presence in the IR transmission spectrum of absorption characteristic of the vibrations of the Ti–O–Ti bond indicates the interaction of the hydrolyzed  $\text{Ti}(\text{OC}_4\text{H}_9)_3\text{OH}$  molecules with each other. The processes passing in FFSs based on Butanol-1–TBT– $\text{SnCl}_4 \cdot 5\text{H}_2\text{O}$  can be represented as follow:



The degree of hydrolysis of titanium(IV) and tin(IV) compounds is insignificant, as evidenced by the change in the kinematic viscosity of FFSs over time ( $T = 20 \pm 2 \text{ }^\circ\text{C}$ ) and their comparison with the viscosity of butanol ( $4.00 \pm 0.03 \text{ mm}^2/\text{s}$  at  $T = 20 \text{ }^\circ\text{C}$ ). As can be seen from Fig. 2, the values the kinematic viscosity of FFSs in the equilibrium region (after 7 days) are close and are in the range from 4.50 (5 mol.% Sn(IV)) to  $4.70 \pm 0.03 \text{ mm}^2/\text{s}$  (30 mol.% Sn(IV)).

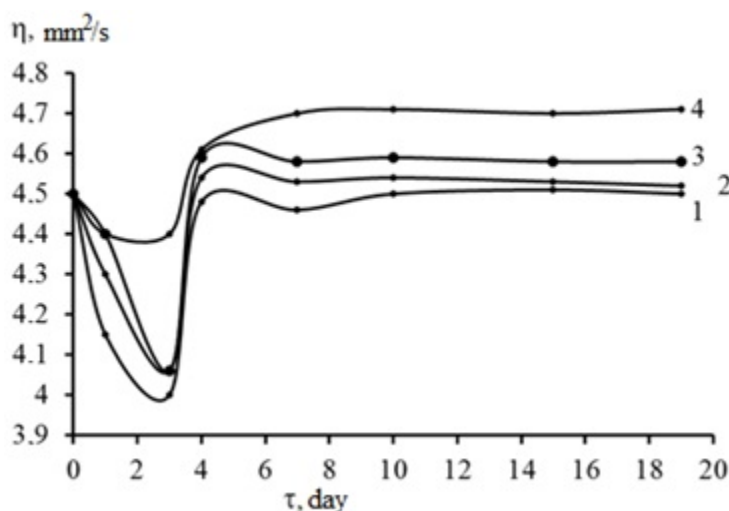


FIG. 2. The change of the kinematic viscosity of FFSs based on Butanol-1–TBT– $\text{SnCl}_4 \cdot 5\text{H}_2\text{O}$ , with different content of Sn(IV) (mol.%): 1–5; 2–15; 3–25; 4–30

Presumably, a decrease of the viscosity of all FFSs in the first three days is associated with the processes of destruction of intermolecular bonds between *n*-butanol molecules [27]. An increase of the viscosity after the third day is explained by the formation of a new structure of the solutions, where bonds are formed between *n*-butanol molecules and hydrolyzed salts, as well as by the formation of  $(\text{C}_4\text{H}_9\text{O})_3\text{Ti} - \text{O} - \text{Ti}(\text{OC}_4\text{H}_9)_3$ . The state of equilibrium in FFSs, in which there is no change in viscosity, is observed after 7 days of keeping the solutions at a temperature of  $20 \text{ }^\circ\text{C}$  and it lasts up to 20 days. At this period of time, FFSs are suitable for the preparation of oxide films with stable properties. An increase in the addition of  $\text{SnCl}_4 \cdot 5\text{H}_2\text{O}$  does not affect the stability of the solution, but insignificantly increases the value of the kinematic viscosity. The increase of the viscosity can be associated with the amount of introduced water with crystalline hydrate, which is involved in the processes of salt hydrolysis and polycondensation. According to the results of the “Spectrum-turbidity” method, all FFSs belong to colloidal systems (sols) and contain colloidal particles with a size of 80–90 nm.

The results of thermal analysis of the dry residue of Butanol-1– $\text{SnCl}_4 \cdot 5\text{H}_2\text{O}$  solution (Fig. 3) indicate that the process of its thermal destruction is characterized by three stages of decomposition and ends at the temperature of about  $350 \text{ }^\circ\text{C}$ . According to the XRD results, the final decomposition product of the dry residue of Butanol-1– $\text{SnCl}_4 \cdot 5\text{H}_2\text{O}$  solution is tin dioxide with a rutile structure (Fig. 4).

As can be seen in Fig. 4, the degree of crystallinity of the sample obtained at a temperature of  $400 \text{ }^\circ\text{C}$  (Fig. 4a) is small and increases with the increase of the annealing temperature up to  $600 \text{ }^\circ\text{C}$  (Fig. 4b).

The results of the analysis of the change in mass on the TG curve of decomposition of the dry residue of Butanol-1– $\text{SnCl}_4 \cdot 5\text{H}_2\text{O}$  solution are presented in Table 1. The loss of mass according to the TG curve at the third stage is 2.79 wt.%. This corresponds to the removal of two water molecules from stannic acid, which is formed at the second stage in the temperature range between 225 and  $285 \text{ }^\circ\text{C}$ . The stannic acid is formed from tin(IV) hydroxychloride crystalline hydrate with an endothermic effect with a maximum of  $244.1 \text{ }^\circ\text{C}$ . It is not possible to determine the composition of the removed products and the initial composition of the dry residue of Butanol-1– $\text{SnCl}_4 \cdot 5\text{H}_2\text{O}$  solution using the TG curve, due to the superposition of the processes of its thermal destruction in the temperature range between 20 and  $225 \text{ }^\circ\text{C}$ . However, the IR spectrum of this sample indicates that it contains not only hydrolyzed tin(IV) salt, but also butanol (Fig. 5).

Therefore, four endothermic effects accompanying the first stage of the thermal decomposition of the dry residue of solution with temperature maxima of 46.8, 76.0, 163.3, and  $190.5 \text{ }^\circ\text{C}$ , can be associated with the removal of molecules

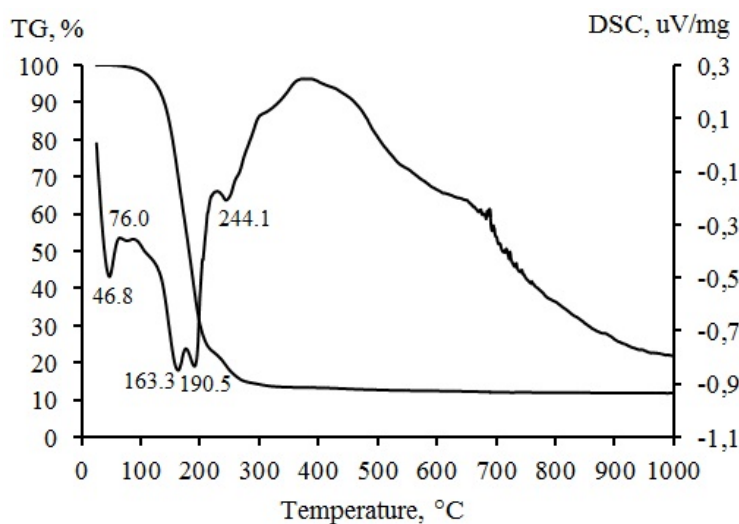


FIG. 3. The thermogram of the decomposition of the dry residue of Butanol-1–SnCl<sub>4</sub>·5H<sub>2</sub>O solution

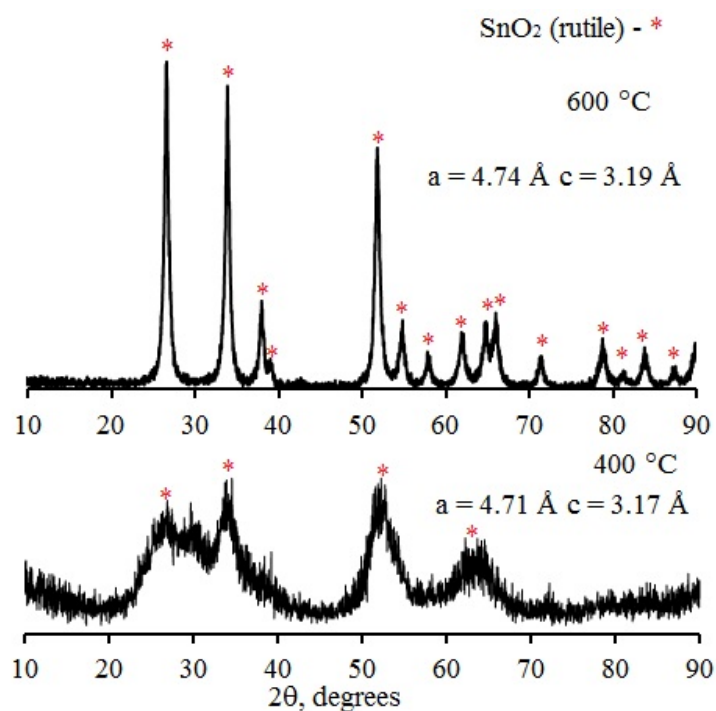
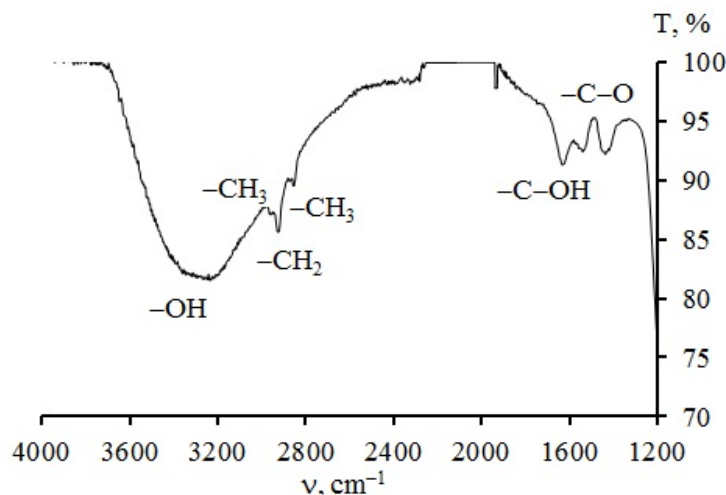


FIG. 4. The diffraction patterns of the dry residue of Butanol-1–SnCl<sub>4</sub>·5H<sub>2</sub>O solution annealed at 400 °C (1 hours) and 600 °C (1 hours)

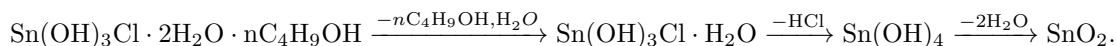
TABLE 1. The results of the analysis of the change in mass on the TG curve of the dry residue of Butanol-1–SnCl<sub>4</sub>·5H<sub>2</sub>O solution

Stage	$T$ , °C	Loss of mass, wt. %	$M$ , g/mol and composition of the removed material practice/theory	$M$ , g/mol and the composition of the resulting material practice/theory
I	20–225	77.13	*	222.85 Sn(OH) <sub>3</sub> Cl·H <sub>2</sub> O/ <b>223.14 Sn(OH)<sub>3</sub>Cl·H<sub>2</sub>O</b>
II	225–285	8.20	36.71 HCl/ <b>36.45 HCl</b>	186.14 Sn(OH) <sub>4</sub> / <b>186.69 Sn(OH)<sub>4</sub></b>
III	285–350	2.79	17.73 H <sub>2</sub> O/ <b>17.99 H<sub>2</sub>O</b>	151.13 SnO <sub>2</sub> / <b>150.69 SnO<sub>2</sub></b>

\*The composition was not determined

FIG. 5. The IR spectrum of the dry residue of Butanol-1-SnCl<sub>4</sub>·5H<sub>2</sub>O solution

of adsorbed water, butanol, and hydrogen chloride, respectively. The scheme of thermal destruction of the dry residue of Butanol-1-SnCl<sub>4</sub>·5H<sub>2</sub>O solution can be represented as follows:



The thermal decomposition of the dry residue of Butanol-1-TBT solution proceeds stepwise with 3 stages (Fig. 6). The first stage proceeds at the temperature range between 25 and 330 °C and is characterized by the maximum change in the mass of the sample. The decomposition process in this temperature range is accompanied by two endothermic effects with maxima of 47.4 and 80.2 °C, as well as the exothermic effect at a temperature of 285.4 °C. The removal of adsorbed butanol and water molecules proceeds with the endothermic effects, and the exothermic effect indicates the burnout of butoxy-groups.

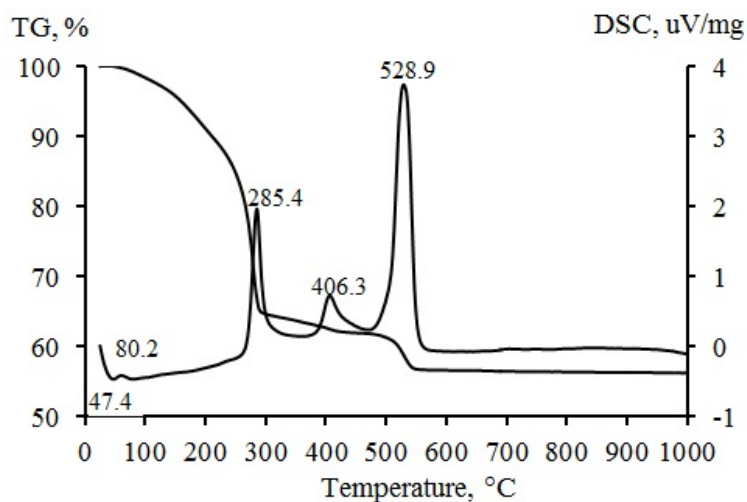


FIG. 6. The thermogram of the decomposition of the dry residue of Butanol-1-TBT solution

The next two stages (330–450 °C – stage II, 450–560 °C – stage III) are accompanied by exothermic effects with maxima at 406.3 and 528.9 °C, respectively. At these stages, further burnout of butoxy-groups occurs and, eventually, at a temperature of 550 °C, titanium dioxide is obtained:



The XRD results indicate that titanium oxide crystallizes in the anatase phase at a given temperature (Fig. 7).

Figure 8 shows the thermogram of decomposition of FFS-60(20 mol.% Sn(IV)) sample. The TG curve indicates four stages of thermal destruction of this sample. The comparison with the thermograms of dry residues of Butanol-1-SnCl<sub>4</sub>·5H<sub>2</sub>O and Butanol-1-TBT solutions indicates that with the combined presence of TBT and tin(IV) chloride in butanol, the temperature regimes of each stage shift to lower temperatures and the decomposition process ends at

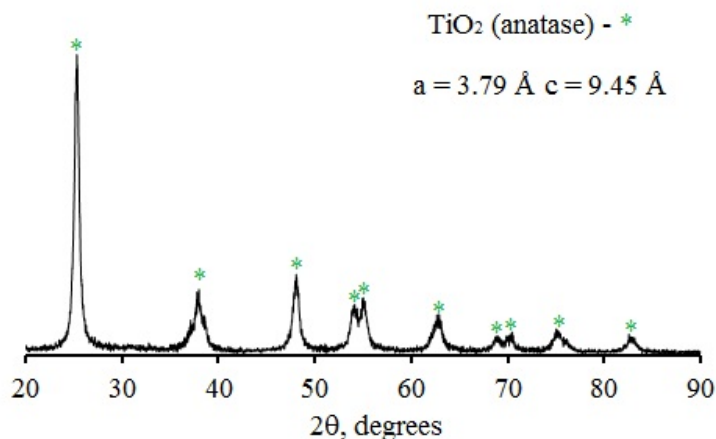


FIG. 7. The diffraction pattern of the dry residue of Butanol-1–TBT solution annealed at 550 °C

the temperature of 500 °C. This is 50 °C lower than the final decomposition temperature of dry residue of Butanol-1–TBT solution. The change in the intensity of the maxima on the DSC curve indicates the superposition of processes accompanied by the removal of hydrogen chloride, water (endothermic effects) with the process of burnout of butoxy-groups (exothermic effects).

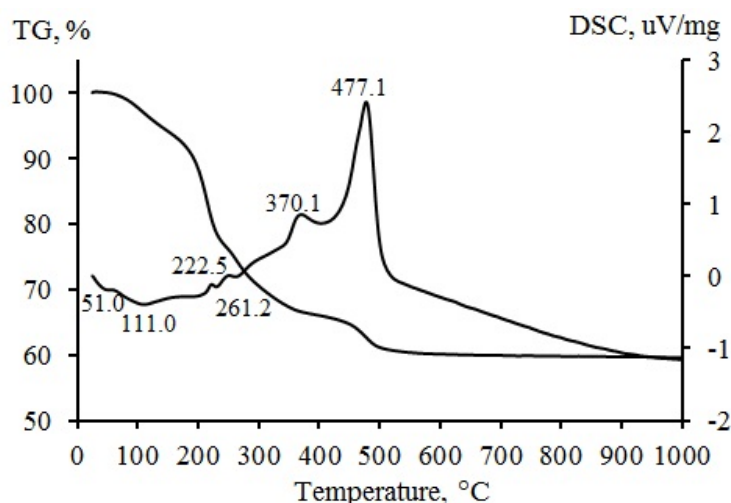


FIG. 8. The thermogram of the FFS-60(20 mol.% Sn(IV)) decomposition

The results of XRD analysis of the FFS-60(30 mol.% Sn(IV)) sample annealed at 500 °C indicate the formation of two substances: TiO<sub>2</sub>:Sn solid solution with an anatase structure and SnO<sub>2</sub> with a rutile structure (Fig. 9). The broad diffraction peaks indicate a low crystallinity of the sample. A decrease in the content of SnO<sub>2</sub> in the composition of the samples from 30 mol.% to 5 mol.% makes it possible to obtain a solid solution of the anatase structure (Fig. 9) from the FFS based on Butanol-1–TBT–SnCl<sub>4</sub>·5H<sub>2</sub>O.

A decrease in the FFS annealing temperature to 300 °C even with increase time of calcination up to 9 hours leads to the formation of X-ray amorphous sample. The elemental composition of such samples was studied based on the results of EDX analysis. The results of analysis of the sample with a content of 10 mol. % Sn(IV) are shown in Fig. 10. As can be seen in Fig. 10, the sample contains the element chlorine, which distributes with the tin over the sample surface. In addition, the sample contains oxygen and titanium.

An increase in the annealing temperature of FFS-60 to 400 °C (9 hours) leads to the formation of TiO<sub>2</sub>:Sn solid solution from FFS-60(5 mol.% Sn(IV)) and a mixture of TiO<sub>2</sub>:Sn solid solution with SnO<sub>2</sub> from FFS-60(30 mol.% Sn(IV)) (Fig. 11).

The formation of TiO<sub>2</sub>:Sn solid solution and a mixture of TiO<sub>2</sub>:Sn solid solution with SnO<sub>2</sub> from FFS based on Butanol-1–TBT–SnCl<sub>4</sub>·5H<sub>2</sub>O is possible at a temperature of at least 400 °C. Titanium dioxide and possibly tin(IV) hydroxychlorides are present in the samples obtained from FFS at 300 °C.

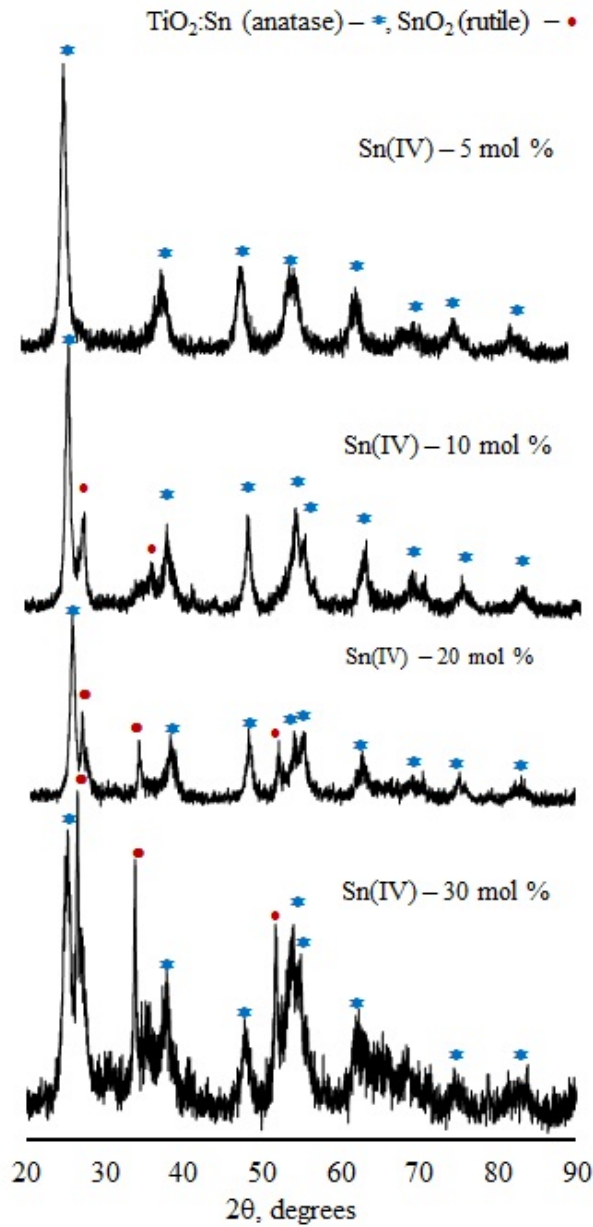


FIG. 9. The X-ray diffraction patterns of samples obtained from FFS-60(5–30 mol.% Sn(IV)) at 500 °C (1 hours)

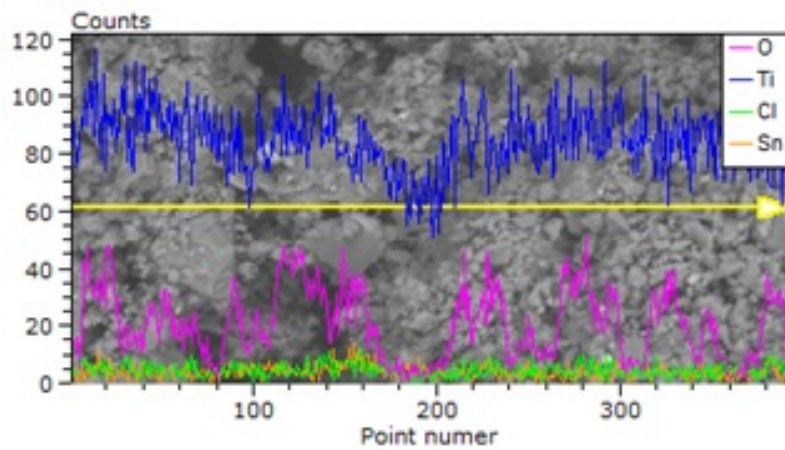


FIG. 10. The distribution of elements over the surface of the sample obtained from the FFS-60(10 mol.% Sn(IV)) at 300 °C (9 hours)

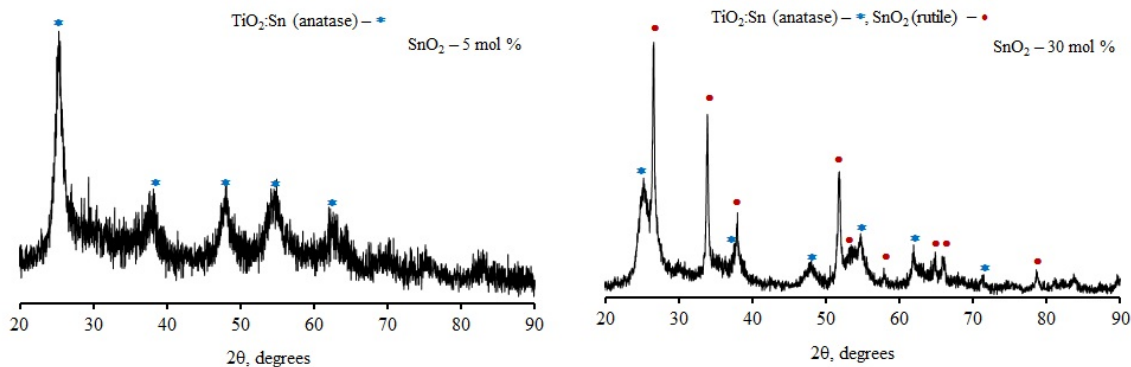


FIG. 11. The XRD patterns of samples obtained from the FFS-60 at 400 °C (9 hours)

### 3.2. Composition and properties of films obtained from FFS based on Butanol-1-TBT-SnCl<sub>4</sub>·5H<sub>2</sub>O

The films were prepared by the sol-gel method on glass substrates using FFSs at annealing temperatures of 60, 300, and 400 °C, respectively. The EDX analysis of films obtained on glass substrates at 400 °C (Fig. 12a) indicates the presence of the maximum emission of the Si, O, Ca, Mg, Na, Al elements of the substrate, as well as Ti, Sn, O elements of the films.

In addition to the emission maxima of the substrate elements, the EDX spectrum of the films annealed at a temperature of 300 °C for 9 hours contains the maxima emission of the Ti, Sn, O, and Cl elements. Consequently, both in the powder state and in the thin-film state, tin(IV) hydroxychlorides do not decompose completely at a temperature of 300 °C. The results of EDX analysis of the films annealed at 300 and 400 °C indicate that oxide phases are formed only at a temperature of 400 °C (Fig 10, 11). It has been shown by scanning electron spectroscopy that oxide films are uniform and continuous regardless of the tin content (Fig. 12b).

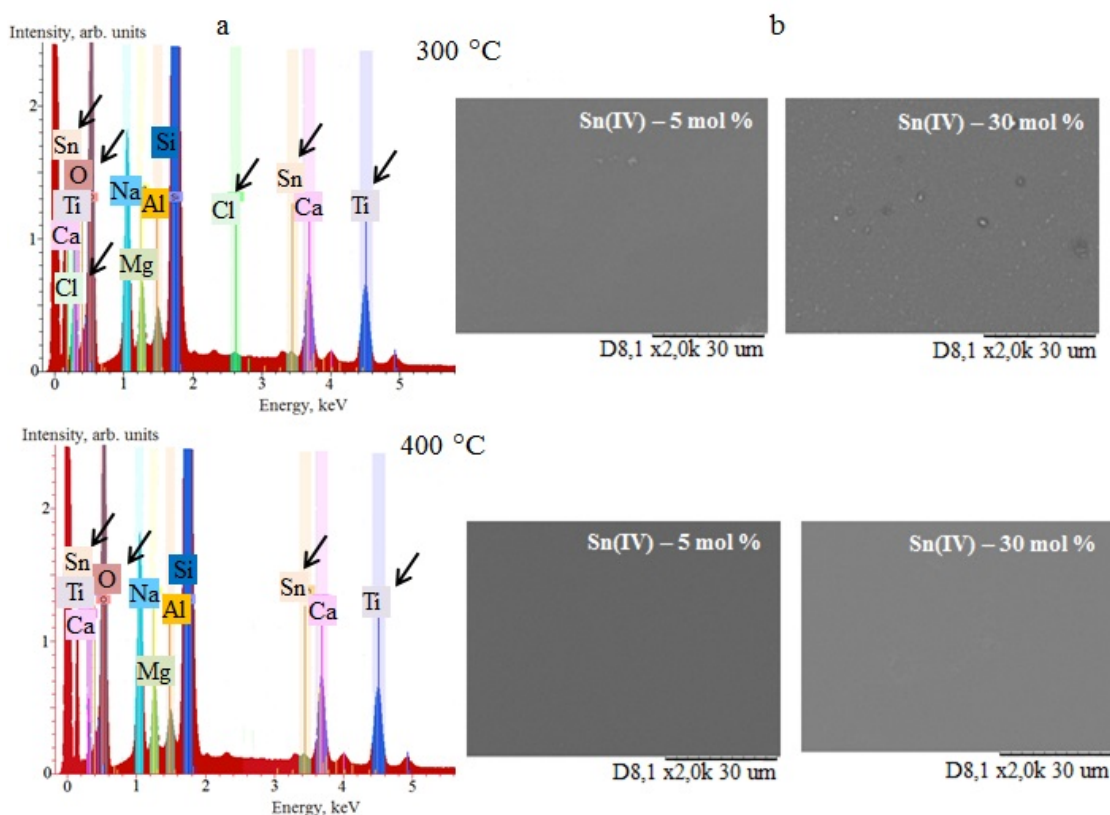


FIG. 12. EDX results (a) and SEM images (b) of the films obtained on glass substrates from FFSs at 300 and 400 °C (9 hours)

Taking into account the conditions and intermediate products of the preparation of TiO<sub>2</sub> with Sn(IV) films, one should expect the presence of amorphous titanic (TiO<sub>2</sub>·nH<sub>2</sub>O) and stannous (SnO<sub>2</sub>·mH<sub>2</sub>O) acids in their IR spectra. The

IR spectra of  $\text{TiO}_2$  with 5 mol.% Sn(IV) films on glass substrates (Fig. 13) annealed at temperatures of 300 and 400 °C confirm the presence of water and hydroxyl groups in the samples. There are broad absorption bands with maxima at  $3270\text{--}3360\text{ cm}^{-1}$ , caused by the vibrations of  $\text{--OH}$  groups. The IR spectra of the films annealed at 600 °C do not contain vibrations of the  $\text{--OH}$  groups. If one take into account the results of XRD analysis of powders obtained at 400 °C (Fig. 11) where the crystalline phase of tin dioxide is recorded, and the diffraction maxima related to the anatase phase are wide enough, it can be assumed that the amorphous titanic acid is present in the films obtained at 300 and 400 °C.

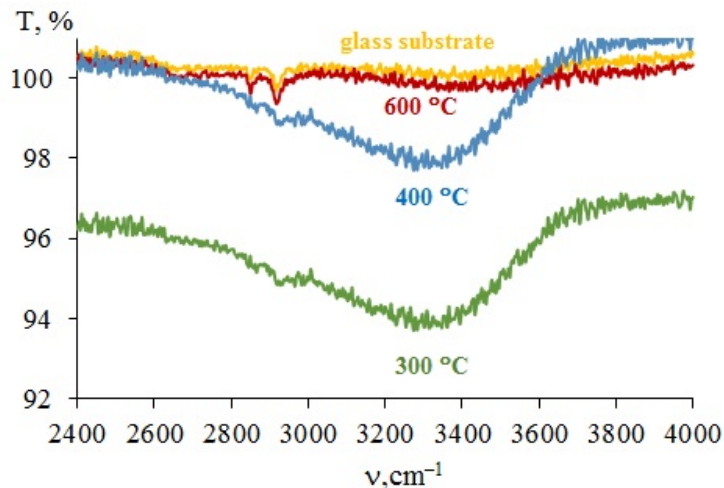


FIG. 13. IR spectrum of pure glass and  $\text{TiO}_2$  with 5 mol.% Sn (IV) films on glass substrates annealed at different temperatures (9 hours)

Table 2 shows the compositions as well as the thickness ( $d$ ), refractive index ( $n$ ), surface resistance ( $R$ ) and the value of the energy level of charge carriers ( $\Delta E_a$ ) of films obtained from FFSs at 400 and 300 °C.

TABLE 2. Compositions and properties of the films

Sn(IV), mol.%/ Properties	0	5	10	20	30
	after annealing at 300 °C				
composition of film	$\text{TiO}_2 \cdot n\text{H}_2\text{O}$	$\text{TiO}_2 \cdot n\text{H}_2\text{O}$ $\text{Sn(OH)}_3\text{Cl}$	$\text{TiO}_2 \cdot n\text{H}_2\text{O}$ $\text{Sn(OH)}_3\text{Cl}$	$\text{TiO}_2 \cdot n\text{H}_2\text{O}$ $\text{Sn(OH)}_3\text{Cl}$	$\text{TiO}_2 \cdot n\text{H}_2\text{O}$ $\text{Sn(OH)}_3\text{Cl}$
$d \pm 0.02$ , nm	48.13	90.21	100.05	105.34	107.86
$n \pm 0.01$	1.89	1.84	1.78	1.73	1.69
$R$ , $\Omega$	$> 10^{10}$	$10^9$	$10^9$	$10^9$	$10^9$
	after annealing at 400 °C				
composition of film	$\text{TiO}_2$ anatase $\text{TiO}_2 \cdot n\text{H}_2\text{O}$	$\text{TiO}_2\text{:Sn}$ anatase $\text{TiO}_2 \cdot n\text{H}_2\text{O}$	$\text{TiO}_2\text{:Sn}$ anatase $\text{SnO}_2$ rutile $\text{TiO}_2 \cdot n\text{H}_2\text{O}$	$\text{TiO}_2\text{:Sn}$ anatase $\text{SnO}_2$ rutile $\text{TiO}_2 \cdot n\text{H}_2\text{O}$	$\text{TiO}_2\text{:Sn}$ anatase $\text{SnO}_2$ rutile $\text{TiO}_2 \cdot n\text{H}_2\text{O}$
$d \pm 0.02$ , nm	48.01	88.14	99.18	102.87	104.15
$n \pm 0.01$	1.89	1.84	1.76	1.72	1.66
$R$ , $\Omega$	$10^{10}$	$10^8$	$10^8\text{--}10^9$	$10^9$	$10^9$
$\Delta E_a$ , eV	–	0.5	0.5	0.9	13

As can be seen in Table 2, the increase of the Sn(IV) content in the composition of the films leads to an increase in their thickness and a decrease in the refractive index. The thickness of the films obtained from FFS depends on the value

of the FFSs viscosity. The viscosity of FFSs increases with an increase of Sn(IV) content and, consequently, the thickness of the films increases with an increase of tin dioxide content in the composition. The decrease in the refractive index is due to the increase in the thickness of the coatings.

The change in the composition of the films with an increase in the temperature of their preparation from 300 to 400 °C practically does not affect the value of the refractive index, but affects the conductivity. All films are highly resistive and electronically conductive. However, the minimum resistance value is characteristic for films that are a solid solution with an anatase structure and with an admixture of the amorphous phase of titanate acid.

The transmittance spectra of TiO<sub>2</sub>, SnO<sub>2</sub> and TiO<sub>2</sub> with Sn(IV) films annealed at 400 °C on glass substrate and spectrum of pure glass are shown in Fig. 14.

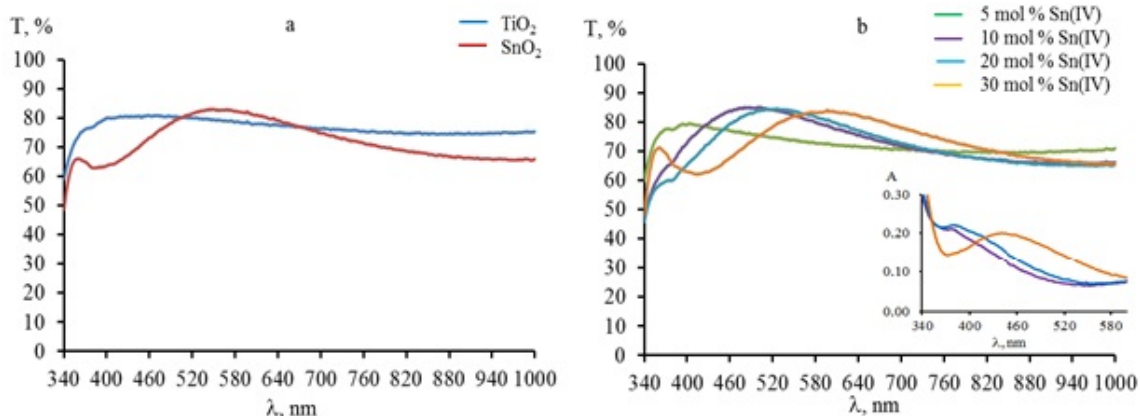


FIG. 14. The transmittance spectra of (a) TiO<sub>2</sub>, SnO<sub>2</sub> films and (b) TiO<sub>2</sub> with Sn(IV) films prepared on the glass substrate at 400 °C

A wide absorption band with a maximum of about 380 nm is present in the spectra of tin dioxide film (Fig. 14a). The appearance of this absorption band is due to the charge transfer Sn(II) → Sn(IV) and the destruction of these centers as a result of the migration of bulk oxygen to the surface. It is assumed that Sn(II) is always present on the surface of SnO<sub>2</sub> [28]. The absorption at 580–600 nm is caused by the presence of oxygen vacancies (single- and double-charged) in SnO<sub>2</sub> [29]. The transmission spectrum of the titanium dioxide film (Fig. 14a) has no maxima or minima and is characterized by a transmission coefficient of 75–80% in the visible light range. The transmission spectrum of films based on a solid solution without tin dioxide (Fig. 14b, 5 mol.% Sn(IV)) impurities is the same as the transmission spectrum for films based on titanium dioxide, which once again confirms the formation of a solid solution in the film samples. The transmittance of these films in the visible light regime of the spectrum is 78–70%. A decrease in the transmittance of films based on a solid solution compared to titanium dioxide films is caused by their greater thickness. A general view of the transmission spectra of films containing 10–30 mol.% Sn(IV) (Fig. 14b) is similar to the transmission spectrum of the SnO<sub>2</sub> film (Fig. 14a). A decrease in the tin(IV) contents (30–10%) in the composition of oxide films leads to a hypsochromic shift of the absorption maximum corresponding to the transition of Sn(II) → Sn(IV) electrons.

#### 4. Conclusion

In this study, the formation of transparent conductive films on glass substrates based on titanium dioxide with 5–30 mol.% Sn(IV) additives by sol-gel method from FFSs based on Butanol-1-TBT-SnCl<sub>4</sub>·5H<sub>2</sub>O and annealed at temperature 300–400 °C (9 hours) has been demonstrated. The content of Sn(IV) influences the composition of films. The solid solution based on titanium dioxide with anatase structure is formed at a content of 5 mol.% Sn(IV); the films with a content of 10–30 mol.% Sn(IV) are the mixture of the TiO<sub>2</sub>:Sn solid solution and SnO<sub>2</sub> with rutile structure. Regardless of the tin content, all films contain an amorphous TiO<sub>2</sub>·nH<sub>2</sub>O phase. The formation of oxide phases occurs through the stages of thermal destruction of Sn(OH)<sub>3</sub>Cl, tin acid, and burnout of butoxy groups of butoxytitanium(IV). In addition to titanate acid, the films obtained at 300 °C contain a tin salt of presumptive of the composition Sn(OH)<sub>3</sub>Cl. The surface resistance of glass decreases by 10<sup>8</sup> times after deposition of the film based on TiO<sub>2</sub> with 5 mol.% Sn(IV) and by 10<sup>7</sup> times after deposition of the film based on TiO<sub>2</sub> with 10–30 mol.% Sn(IV). The transparency coefficient of films based on TiO<sub>2</sub> with 5 mol.% Sn(IV) in the entire visible light range of the spectrum is 80–70%, the maximum transmittance of 78–85% of the films based on TiO<sub>2</sub> with 10, 20 and 30 mol.% Sn(IV) are at wavelengths of 423–745 nm, 452–734 nm and 505–830 nm, respectively. The Sn(IV) additive up to 5 mol. % in the TiO<sub>2</sub>: Sn solid solution is the key to successfully obtaining a transparent conductive coating that can be used as a photoelectrode in dye-sensitized solar cells.

## References

- [1] Abudayyeh O.K., Chavez A., Han S.M., Rounsaville B., Upadhyaya V. and Rohatgi A. Silver-carbon-nanotube composite metallization for increased durability of silicon solar cells against cell cracks. *Sol. Energy Mater. Sol. Cells.*, 2021, **225**, 111017.
- [2] Ramprabhu R., Sanjay K., Saran Kumar V., Santhosh A.C., Saravanan M. and Ajayan J. An overview of recent developments in silicon solar cells. *ICACCS*, 2019, P. 1120–1122.
- [3] R.H.E. Hassanien, M. Li and F. Yin. The integration of semi-transparent photovoltaic on greenhouse roof for energy and plant production. *Renew. Energ.*, 2018, **121**, P. 377–388.
- [4] Das P., Sengupta D., Kasinadhuni U., Mondal B. and Mukherjee K. Nano-crystalline thin and nano-particulate thick TiO<sub>2</sub> layer: Cost effective sequential deposition and study on dye sensitized solar cell characteristics. *Mater. Res. Bull.*, 2015, **66**, P. 32–38.
- [5] Fitra M., Daut I., Irwanto M., Gomesh N. and Irwan Y.M. Effect of TiO<sub>2</sub> thickness Dye Solar Cell on charge generation, *Energy Procedia, Energy Procedia*, 2013, **36**, P. 278–286.
- [6] Winkless L. Could dye-sensitized solar cells work in the dark. *Mater. Today*, 2017, **20**, 289.
- [7] Blakers A., Zin N., McIntosh K.R. and Fong K. High efficiency silicon solar cells. *Energy Procedia*, 2013, **33**, 1–10.
- [8] Wang W.W., Zhu Y.J. and Yang L.X. ZnO-SnO<sub>2</sub> Hollow Spheres and Hierarchical Nanosheets: Hydrothermal Preparation, Formation Mechanism, and Photocatalytic Properties. *Adv. Funct. Mater.*, 2007, **17**, P. 59–64.
- [9] Li N., Du K., Liu G., Xie Y., Zhou G., Zhu J., Li F. and Cheng H.-M. Effects of oxygen vacancies on the electrochemical performance of tin oxide. *J. Mater. Chem. A*, 2013, **1**, P. 1536–1539.
- [10] Yang L., Yang Y., Liu T., Ma X., Lee S.W. and Wang Y. Oxygen vacancies confined in SnO<sub>2</sub> nanoparticles for glorious photocatalytic activities from the UV, visible to near-infrared region. *New J. Chem.*, 2018, **42**, P. 15253–1526.
- [11] Domashevskaya E.P., Ryabtsev S.V., Tutov E.A., Yurakov, Chuvenkova O.A.Y.A., Lukin A.N. Optical properties of SnO<sub>2-x</sub> nanolayers. *Tech. Phys. Lett.*, 2006, **32**, P. 782–784.
- [12] Senevirathna M.K.I., Pitigala P.K.D.P., Premalal E.V.A., Tennakone K., Kumara G.R.A. and Konno A. Stability of the SnO<sub>2</sub>/MgO dye-sensitized photoelectrochemical solar cell. *Sol. Energy Mater. Sol. Cells*, 2007, **91**, P. 544–547.
- [13] C. Kılıç and Zunger A. Origins of Coexistence of Conductivity and Transparency in SnO<sub>2</sub>. *Phys. Rev. Lett.*, 2002, **88**(9), 95501.
- [14] Snaith H.J. and Ducati C. SnO<sub>2</sub>-based dye-sensitized hybrid solar cells exhibiting near unity absorbed photon-to-electron conversion efficiency. *Nano Lett.*, 2010, **10**(4), P. 1259–1265.
- [15] Li Y., Zhu J., Huang Y., Liu F., Lu M., Chen S., Hu L., Tang J., Yao J., Dai S. Mesoporous SnO<sub>2</sub> nanoparticle films as electron-transporting material in perovskite solar cells. *RSC Adv.*, 2015, **5**, 28424–28429.
- [16] Ke W., Fang G., Liu Q., Xiong L., Qin P., Tao H., Wang J., Lei H., Li B., Wan J., Yang G., Yan Y. Low-temperature solution processed tin oxide as an alternative electron transporting layer for efficient perovskite solar cells. *J. Am. Chem. Soc.*, 2015, **137**, P. 6730–6733.
- [17] Xie H., Yin X., Liu J., Guo Y., Chen P., Que W., Wang G. and Gao B. Low temperature solution-derived TiO<sub>2</sub>-SnO<sub>2</sub> bilayered electron transport layer for high performance perovskite solar cells. *Appl. Surf. Sci.*, 2019, **464**, P. 700–707.
- [18] Pitchai S., Eswaramoorthy N., Natarajan M., Santhanam A., Ramakrishnan V.M., Asokan V., Palanichamy P., Palanisamy B., Kalimuthua A. and Velauthapillaib D. Interfacing green synthesized flake like-ZnO with TiO<sub>2</sub> for bilayer electron extraction in perovskite solar cells. *New J. Chem.*, 2020, **44**, P. 8422–8433.
- [19] Gambhire A.B., Lande M.K., Kalokhe S.B., Shirsat M.D., Patil K.R., Gholap R.S. and Arbad B.R. Synthesis and characterization of high surface area CeO<sub>2</sub>-doped SnO<sub>2</sub> nanomaterial. *Mater. Chem. Phys.*, 2008, **112**, P. 719–722.
- [20] Bose A.C., Kalpana D., Thangadurai P. and Ramasamy S. Synthesis and characterization of nanocrystalline SnO<sub>2</sub> and fabrication of lithium cell using nano-SnO<sub>2</sub>. *J. Power Sources.*, 2002, **107**, P. 138–141.
- [21] Yang Y., Zhang Q., Zhang B., Mi W.B., Chen L., Li L., Zhao C., Diallo K.E.M. and Zhang X.X. The influence of metal interlayers on the structural and optical properties of nano-crystalline TiO<sub>2</sub> films. *Appl. Surf. Sci.*, 2012, **258**, P. 4532–4537.
- [22] Kaleji B.K. and Sarraf-Mamoory R. Nanocrystalline sol-gel TiO<sub>2</sub>-SnO<sub>2</sub> coatings: preparation, characterization and photo-catalytic performance. *Mater. Res. Bull.*, 2012, **47**, P. 362–369.
- [23] Medjaldi F., Bouabellou A., Bouachiba Y., Taabouche A., Bouatia K. and Serrar H. Study of TiO<sub>2</sub>, SnO<sub>2</sub> and nanocomposites TiO<sub>2</sub>:SnO<sub>2</sub> thin films prepared by sol-gel method: Successful elaboration of variable-refractive index systems. *Mater. Res. Express.*, 2020, **7**, 016439.
- [24] Jalava J., Taavitsaine V., Haario H. and Lamberg L. Determination of particle and crystal size distribution from turbidity spectrum of TiO<sub>2</sub> pigments by means of t-matrix. *J. Quant. Spectrosc. Radiat. Transfer*, 1998, **60**, P. 399–409.
- [25] Zhrebtsov D.A., Kuznetsov G.F., Kleshchev D.G., Syutkin S.A., Pervushin V.Y., German V.A., Viktorov V.V., Kolmogortsev A.M. and Serikov A.S. Characteristics of the hydrous titanium dioxide-anatase phase transformation during hydrothermal treatment in aqueous solutions. *Russ. J. Inorg. Chem.*, 2010, **55**, P. 1197–1201.
- [26] Jackson P. and Parfitt G.D. Infra-red study of the surface properties of rutile adsorption of ethanol, n-butanol and n-hexanol. *J. Chem. Soc. Faraday Trans. I.*, 1972, 1443.
- [27] Erdei-Gruz T. *Transfer Phenomena in Water Solutions*. John Wiley & Sons, New York, 1974, 512 p.
- [28] Batzill M. and Diebold U. The surface and materials science of tin oxide. *Progress in Surface Science*, 2005, **79**, P. 47–154.
- [29] Popescu D.A., Herrmann J., Ensuque A. and Bozon-Verduraz F., Nanosized tin dioxide: Spectroscopic (UV-VIS, NIR, EPR) and electrical conductivity studies. *Phys. Chem. Chem. Phys.*, 2001, **3**, P. 2522–2530.

---

Submitted 1 February 2022; revised 18 April 2022; accepted 19 April 2022

## Information about the authors:

S. Kuznetsova – National Research Tomsk State University, Lenin, 36, Tomsk, 634050, Russia; onm@mail.tsu.ru

O. Khalipova – National Research Tomsk State University, Lenin, 36, Tomsk, 634050, Russia;

Yu-Wen Chen – Department of Chemical Engineering, National Central University, Jhongli 32001, Taiwan;

V. Kozik – National Research Tomsk State University, Lenin, 36, Tomsk, 634050, Russia;

**Conflict of interest:** the authors declare that they have no known competing financial interests or personal relationships that have influenced the work reported in this paper.